

Microenvironments at Specific Chain Sites in Polystyrene Solutions Studied by Photoisomerization and Computer Simulation[†]

You Shin Kim and Chong Sook Paik Sung*

Polymer Science Program, Institute of Materials Science, University of Connecticut, 97 North Eagleville Road, Storrs, Connecticut 06269-3136

Young-Hwa Kim

Higher Dimension Research, Inc., 7650 Currell Boulevard, St. Paul, Minnesota 55125

Received April 12, 1995; Revised Manuscript Received June 20, 1995[®]

ABSTRACT: Microenvironments of polystyrene solutions are investigated as a function of polymer concentration and the nature of solvent both by computer simulation and by the rate of the photoisomerization of azobenzene, attached to specific sites of a polystyrene chain. The sites investigated are the chain center (CPS), the chain end (EPS), and the side chain (SPS). A low molecular weight azobenzene analog (4-phenylazoaniline) is studied for comparison. From the simulated site-specific segment-density distributions, it is confirmed that the chain ends are located further away from the center of mass than other chain sites. From the simulated site-specific radial distribution functions, it is shown that the local environment is more congested near the chain center than near the chain ends in a dilute Θ solution but approaches a similar environment with increasing concentration. In a good solvent, the local environment is less crowded for both sites than in the Θ solvent, up to 40% concentration. The segment density near the chain center rises more slowly than at the chain end. The *trans* \rightarrow *cis* photoisomerization behavior of azobenzene in polystyrene solutions represents qualitatively the same trend found in computer simulation. While the free probe in the polystyrene/toluene solution has no difficulty in photoisomerizing up to 50% by weight, the three labeled polystyrenes show significant site dependency. Up to 10% solution in toluene, all three labeled polymers experience little difficulty. From 10% to 50%, however, SPS experiences the most difficulty, followed by EPS. CPS is least affected. In cyclohexane (Θ solvent), CPS and SPS experience some difficulty even in dilute solutions. Overall, photoisomerization in a Θ solvent is more difficult than in a good solvent. These results have been interpreted on the basis of the results of computer simulation.

Introduction

Recent theories of polymer solutions such as the mean field theory¹ and renormalization group theory² predict that polymer solutions behave differently depending on the polymer concentration regime. For instance, polymer chains in a good solvent are swollen in a dilute regime because of the excluded-volume effect. As the polymer concentration increases, the excluded-volume effect is screened and disappears, resulting in smaller chain dimensions which eventually approach their unperturbed values. The theoretical predictions have been experimentally confirmed by small-angle neutron scattering (SANS).³ With increasing polymer concentration, a polymer chain experiences a great change in its microenvironment due to chain overlap, interpenetration, and chain contraction. One of the factors which represent the change in microenvironment is the degree of chain interpenetration, which is a significant variable for thermodynamic and hydrodynamic properties of polymer solutions.

Several experimental approaches were developed to determine the degree of interpenetration in polymer solutions such as viscosity,⁴ small-angle neutron and X-ray scattering,⁵ and photophysical techniques.⁶ Using fluorescence energy transfer of rapidly frozen mixtures of donor and acceptor labeled polymers after removal of the frozen solvent by sublimation, Chang and Morawetz^{6b} attempted to characterize the extent of flexible chain interpenetration as a function of concen-

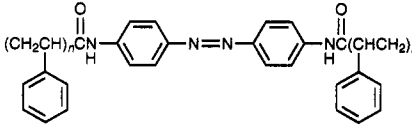
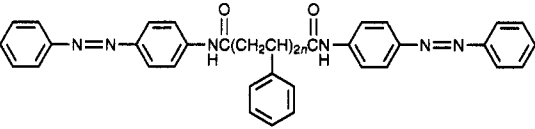
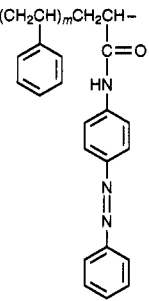
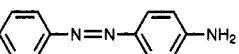
tration and the nature of the solvent. It was found that the extent of interpenetration increases with increasing solvent power of the medium, contrary to the Flory-Krigbaum theory. Hayashi et al.⁷ studied microenvironments of polymer solutions using the twisted intramolecular charge-transfer (TICT) phenomenon which is sensitive to local polarity and segment mobility. They found that the TICT phenomenon of the dimethylamino (DMA) group attached to PMMA as a side group was sensitive to the change in chain dimension due to the nature of the solvent.

In this study, the local environment of polymer chains in solution was investigated both by computer simulation and by the photoisomerization of azobenzene labels at specific chain sites. From the computer simulation, the probability of finding a specific site (e.g. chain end or chain center) of the isolated polymer chain from the center of mass was estimated. In addition, the segmental density near the specific site was calculated as a function of polymer concentration as well as solvent power. These results were used to understand the photoisomerization behavior of azobenzene labels in polymer solution. The photoisomerization of azobenzene was extensively investigated in polymeric solids.^{8,10} The sensitivity of the label to the local free volume has been utilized to probe several phenomena in polymer solids. Using site-specifically labeled polystyrenes with azobenzene, Yu et al. studied their photoisomerization behavior to investigate the effect of physical aging on the free volume distribution of polystyrene film.^{8b} It was found that the fast fraction of photoisomerization of azobenzene could represent the populations of regions having free volume greater than the critical size needed

[†] This paper is dedicated on the happy occasion of the 80th birthday of Professor Herbert Morawetz.

[®] Abstract published in *Advance ACS Abstracts*, August 1, 1995.

Table 1. Chemical Structures and Characteristics of Three Azobenzene-Labeled Polystyrenes and Free Probe

sample	M_w	M_n	T_g (°C)
(1) center-labeled PS (C-PS)	84 000	80 000	100
			
(2) end-labeled PS (E-PS)	92 000	79 000	100
			
(3) side-labeled PS (S-PS)	39 000	26 000	100
			
(4) free probe			
			

for isomerization. This suggests that photoisomerizable labels are able to provide information on the local free volume distribution in their vicinity in a bulk polymer. However, there is not much information reported on the photoisomerization behavior in polymer solutions, especially in concentrated solutions. By studying such behavior as a function of polymer concentration and solvent power, we hope to gain some insight into the change in the microenvironment at specific chain sites in polymer solution as the chain interpenetration increases.

Experimental Procedures

Computer Simulations. Molecular dynamics simulation was carried out at Higher Dimension Research Inc. A long flexible polymer was modeled as a chain of fifty segments connected linearly, while a solvent molecule is modeled as composed of two segments. Lennard-Jones potentials were used for the interactions between segments, assuming a spring type interaction along the chain backbone. Using the customary periodic boundary conditions, a series of molecular dynamics simulations were performed with a certain number of segments, 1 atmospheric pressure, and 300 K for temperature. The simulation was carried out in two stages. In the first stage, the system with initial segment positions was equilibrated. The total potential energy, the radius of gyration of the polymers, and the total radial distribution functions of all segments were computed during the first stage. When these variables reach steady-state values that are consistent with the experimental values obtained from well-equilibrated liquid polymers,⁹ the first stage is completed. In the second stage, the various properties of the system that depend on the energetics of interaction, the concentration of the polymer, and the solvent were computed. These are properties which depend only on "meso" scale features of the polymer and solvent. The meso scale is greater than the atomic scale, yet smaller than the macroscopic scale. Among the various properties of the system computed, we used the segment-density distribution functions and the radial distribution functions at the specific chain sites such as the chain end and

chain center as a function of polymer concentration and solvent power.

Materials and Sample Preparation. The azobenzene chromophore was attached to the specific chain sites of polystyrene such as the chain center (CPS) in the chain backbone, the chain end (EPS), or randomly distributed in the side chain (SPS). Table 1 provides the chemical structures and some characteristics of the three labeled polymers, while the syntheses and purification of three labeled polystyrenes were described elsewhere.¹⁰ A free probe molecule (FP), 4-phenylazoaniline purchased from Aldrich Chemical Co., was recrystallized from toluene and acetone. Toluene and cyclohexane from Fischer were used without further purification. For dilute solutions, a certain amount of each labeled polymer or free probe was dissolved in toluene or cyclohexane to obtain the initial optical density of the trans isomer peak in the range 0.7–1.2. The concentration (by weight) for CPS, EPS, SPS, or free probe was 0.46%, 0.23%, 0.69%, or $1.15 \times 10^{-3}\%$, respectively. These dilute solutions did not contain any unlabeled polystyrene (PS). For concentrated solutions in the range 5%–50% by weight, a certain amount of unlabeled monodisperse PS purchased from Pressure Chemical Co. ($M_w = 90\,000$ for FP, CPS, or EPS while $M_w = 35\,000$ for SPS) was added to the respective dilute solution and dissolved in an ultrasonic bath for several hours. For the study of the effect of the solvent power on the photoisomerization, toluene or cyclohexane was chosen as the good or Θ solvent, respectively. The concentration range studied for the PS/toluene system was up to 50% by weight. Because of the lower boiling point of cyclohexane, a 30% solution was the highest concentration investigated for the PS/cyclohexane system.

Photoisomerization Studies. A flash light source from Photochemical Research Associates (Model 6100A) was used to irradiate the sample to induce trans \rightarrow cis photoisomerization. The lamp intensity was checked regularly with a power meter (Model Scientech 365) and also by measuring the photoisomerization rate with a standard dilute EPS solution in toluene. Interference filters were used to match the irradiation wavelength band with the absorption maximum of each label or probe. UV-visible spectra of the sample were

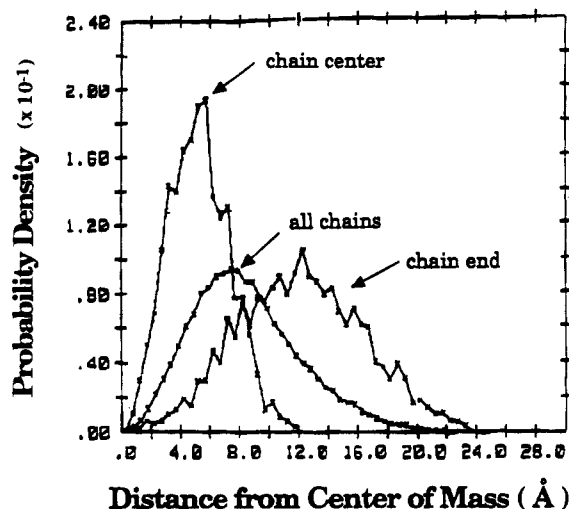


Figure 1. Simulated specific segment-density distribution functions as a function of the distance from the center of mass in dilute solutions.

taken with a Perkin-Elmer diode-array spectrometer (Model 3840) with a Model 7500 data station immediately following a certain number of flashes. The sample in a quartz cell (fluorescence cuvette) was positioned at the intersection point of the analyzing beam and the irradiating beam. All experiments in this study were undertaken at 34.8 ± 0.2 °C which is the Θ temperature for the polystyrene solution in cyclohexane. The photoisomerization reaction was undertaken in a box to minimize interference from background light.

Results and Discussion

1. Molecular Dynamics Simulations. Molecular dynamics simulation has been undertaken to obtain the specific segment-density distributions and the radial distribution functions of polymer chains. It is possible to analytically obtain the distribution function of a specific site from the center of mass based on the assumption of a Gaussian chain.¹¹ This model, however, is not realistic because it does not take into account the so-called excluded volume effect as well as the short-range interaction such as restrictions in bond angle and rotation angle owing to steric hindrance. In molecular simulations, these effects were taken into account. Figure 1 shows the result of such a simulation. For this simulation, 100 chains, each consisting of 50 segments, were used, occupying 10% of the volume. They are assumed to simulate isolated chains. The probability density of finding a segment is plotted as a function of distance from the center of mass. This simulation shows that the end segments are located furthest from the center of mass, while the chain center is nearest to the center of mass. The same conclusion is obtained from the analytical solution.¹¹

In order to see how the segment densities in the vicinity of specific chain sites change with increasing polymer concentration, the specific radial distribution functions for the chain center and the chain end were obtained as a function of the polymer concentration (up to 50% by volume) and the nature of the solvent. Parts a and b of Figure 2 show the plots of the first peak height of the specific segment radial distribution function versus the polymer concentration for the Θ solvent and the good solvent cases, respectively. In the case of the Θ solvent as illustrated in Figure 2a, the chain center has initially a higher segment density since it is closer to the center of mass. With increasing polymer concentration, the segment densities rise slowly for both

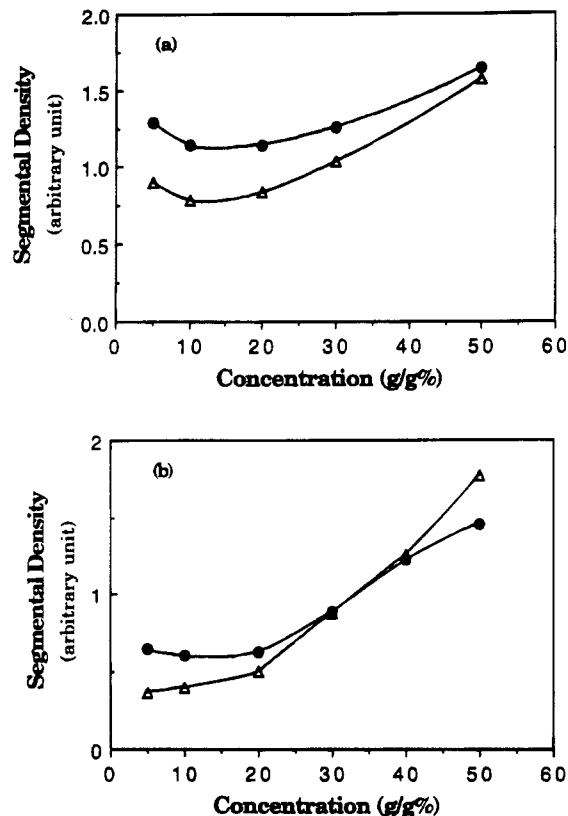


Figure 2. Specific segment densities in the vicinity of the chain center or chain end as a function of polymer concentration: (a) in a Θ solvent; (b) in a good solvent; (Δ) chain end; (\bullet) chain center.

the chain end and the chain center segments. However, the slope of the increase is greater for the chain end than for the chain center. This is reasonable because the chain overlap is expected to occur from the outer shell of the chain coil where the chain ends are located with higher probability, as shown in Figure 1. Such a trend has indeed been verified by computer simulation by Olaj and Zifferer.¹² The microenvironment near the specific segment becomes similar at the concentration of 50% by volume which is larger than the chain overlapping concentration, C^* , of 45% in this system.

The polymer-solvent interaction is made somewhat stronger to see how this behavior changes with increasing solvent power. As illustrated in Figure 2b, in the good solvent case, the segment densities near each site are lower initially in comparison to those in the Θ solvent case. This is reasonable in view of the chain expansion in a good solvent. With increasing polymer concentration, the segment density increases more sharply near the chain end than near the chain center. In fact, there is a crossover point in the good solvent around 30% which is even below the overlap concentration. Beyond 30%, the segment density is greater near the chain end than near the chain center.

2. Photoisomerization in a Good Solvent. It is known that the photoisomerization rate of azo chromophores depends strongly on the free volume in chromophore's vicinity.¹³ The photoisomerization of azobenzene-labeled polystyrenes at specific sites was studied to investigate the microenvironments of polymer solutions as a function of polymer concentration and solvent power. Figures 3 illustrates UV-vis spectra of the dilute solution of the end-labeled polystyrene in toluene (0.23% by weight) as a function of photoisomerization at 34.8 °C. Other labeled polystyrenes and the

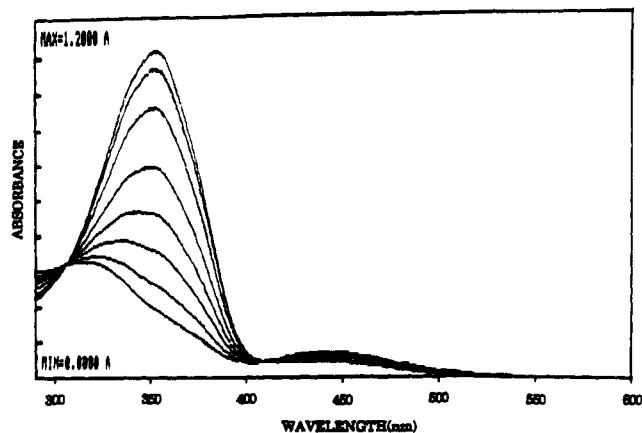


Figure 3. Change of UV-visible spectra of EPS in toluene (0.23% by weight) as a function of photoisomerization at 34.8 °C. From top to bottom, the number of flashes corresponds to 0, 10, 30, 70, 110, 150, 230, and 310.

probe in dilute toluene solution showed similar spectral changes with photoisomerization. As in the previous study,^{9b} the absorption maximum for the trans isomer before irradiation was at 353 nm for the end and the side label, 375 nm for the center label, and 377 nm for the free probe. With an increasing number of irradiation flashes, the absorption peak of the trans isomer decreases, while the cis isomer absorption peak around 325 nm increases. The absorption at 445 nm increases with irradiation since the extinction coefficient at 455 nm, due to the $n \rightarrow \pi^*$ transition of the azo bond, is greater for the cis than for the trans isomer. The cis isomer content at the photostationary state is estimated as about 90% for all the labels and the probe, after subtraction of the cis peak from the trans peak. For the present analysis of the photoisomerization kinetics, only the first 50% of the reaction has been considered in order to reduce the error due to the contribution of the cis isomer. The following equations are used to analyze the kinetics of photoisomerization.¹⁴

$$I(\delta) = \left(1 + \frac{D_\infty}{2} + \frac{D_\infty^2}{12}\right) \ln |\delta| - \left(\frac{1}{2} + \frac{D_\infty}{6}\right) \delta + \frac{\delta^2}{24} = -At + \text{const} \quad (1)$$

$$I'(\delta) = \text{const} - I(\delta) = At \quad (2)$$

Here $\delta = D_\infty - D$ and D_∞ and D are the optical densities in the photostationary state and after t flashes, respectively, and A is equal to $I_0 \phi_t \epsilon_t / y_\infty$, where I_0 is the irradiation intensity, ϕ_t is the quantum yield of photoisomerization, ϵ_t is the molar extinction coefficient of the trans isomer, and y_∞ is the fraction of cis isomer at the photostationary state. The plots of $I'(\delta)$ vs t for the dilute solutions of all three labeled polystyrenes and free probe are illustrated in Figure 4. From the slopes of such plots, the relative rate constants of photoisomerization are obtained. Table 2 summarizes such rate constants for the three labels and the free probe in dilute solutions. These values are smaller than our previously reported values,^{8b} probably due to the lower intensity of the light source (I_0) used for irradiation. However, the trend that the relative rates (A) appear to be greater for the center label and the free probe than for the end and side labels is still the same. This may be due to wavelength dependency of the flash lamp intensity and the transmittance characteristics of the interference filters. Also the similarity in the rates of photoisomer-

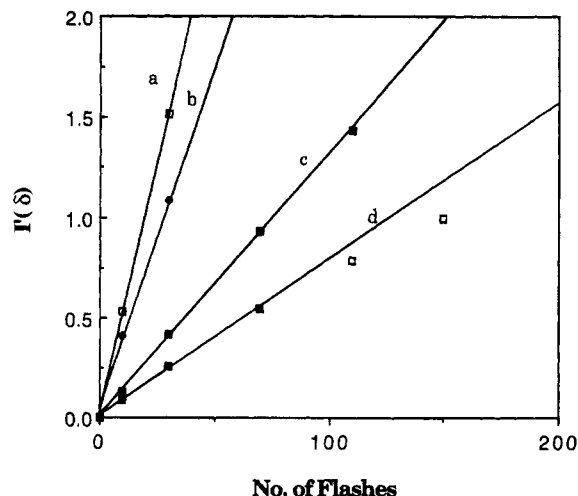


Figure 4. Kinetic plots of photoisomerization of the azobenzene-labeled polystyrenes and the free probe in dilute toluene solutions: (a) C-PS; (b) free probe; (c) E-PS; (d) S-PS.

Table 2. Kinetic Parameters of Three Labeled Polystyrenes and Free Probe in Dilute Toluene Solutions

sample	$10^2 A \text{ (s}^{-1}\text{)}^a$	sample	$10^2 A \text{ (s}^{-1}\text{)}^a$
C-PS	5.034	S-PS	0.783
E-PS	1.308	probe	3.396

^a A is the slope from Figure 4.

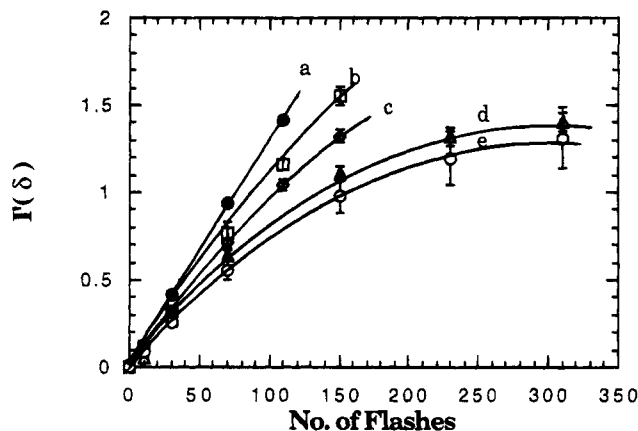


Figure 5. Kinetic plots of photoisomerization of the end-labeled polystyrene in toluene at 34.8 °C as a function of polymer concentration: (a) 0.23%, (b) 15%, (c) 30%, (d) 35%, (e) 50% by weight.

ization of the center label and the free probe shows that the rates of hindered rotation are similar around a bond in the middle of a polymer chain and in its low molecular weight analog, as clearly shown in Liao and Morawetz by the fluorescence excimer technique.^{6c}

Photoisomerization of the labels in moderately concentrated solutions is found to be slower than the analogous process in dilute solutions. Figure 5 shows the kinetic plot of the photoisomerization of EPS in toluene at 34.8 °C as a function of concentration. While the kinetic plot of the dilute solution is linear, the plots of more concentrated solutions are strongly curved, suggesting a dispersion of the rate constant.

To analyze a non-first-order behavior, a biphasic process consisting of fast and slow processes was fitted with the following equation^{8a}

$$e^{-I'(\delta)} = \alpha e^{-A_1 t} + (1 - \alpha) e^{-A_2 t} \quad (3)$$

where t is the number of flashes, A_1 and A_2 are the rate

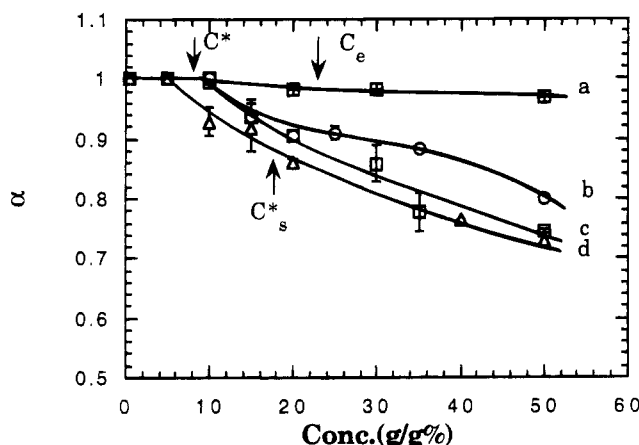


Figure 6. Changes in the fraction of the fast photoisomerization, α , as a function of concentration for the three labeled polystyrenes and the free probe in toluene at 34.8 °C: (a) free probe; (b) C-PS; (c) E-PS; (d) S-PS. C^* and C_e correspond to the free probe, C-PS, and E-PS cases, while C_s^* refers to the S-PS case.

Table 3. Kinetic Parameters Based on Eq 3 for Photoisomerization of End-Labeled PS in Toluene Solutions

conc (wt %)	α	$10^2 A_1$ (s ⁻¹)	$10^5 A_2$ (s ⁻¹)
15	0.94	1.10	1.10
30	0.86	1.28	1.10
35	0.78	1.29	1.10
50	0.75	1.20	1.10

constants for the fast and slow processes, respectively, and α is the fraction of the fast species. When this equation is applied to dilute solutions in a good solvent, α is equal to 1 except for the SPS case, where α is 0.86. Therefore, the value for the SPS was normalized by the α value of the dilute solution in toluene. Table 3 summarizes the kinetic parameters (α , A_1 , and A_2) based on eq 3 for the end label as a function of concentration at 34.8 °C. We note from Table 3 that the values of A_1 and A_2 differ by approximately 3 orders of magnitude and they remain constant with increasing polymer concentration within experimental error. The photoisomerization results from the other labels and the free probe were also analyzed. The values of A_1 and A_2 are about the same order of magnitude for all the samples.

Figure 6 shows the plot of α values as a function of the concentration for the three labels as well as the free probe in toluene at 34.8 °C. The free probe shows little reduction in photoisomerization in toluene up to 50% by weight of polymer. In this concentration range, the free probe which is dispersed uniformly in polymer solution could easily find free volume larger than the critical value required for trans \rightarrow cis isomerization. However, the three labeled polymers show significant site dependency. Up to 10% solution in toluene, all three polymers experience little difficulty. It is worth noting that, as shown in Figure 6, the overlap concentration, C^* , is 8.1% for the free probe, EPS, and CPS. For the SPS, due to its lower molecular weight, C^* is 17.0%. The overlapping concentration C^* is estimated by eqs 4^{15a} and 5,^{15b} where ρ_s is the density of solvent,

$$C^* = \frac{1}{N_A \rho_s} \frac{M_w}{R_g^3} \quad (4)$$

$$R_g = 1.45 \times 10^{-9} M_w^{0.595} \text{ (cm)} \quad (5)$$

N_A is the Avogadro number, M_w is the weight average molecular weight of the polymer, and R_g is the radius of gyration. Equation 5 describes the relationship between R_g and M_w for polystyrene in benzene which is comparable to this system.

The results in Figure 6 show that the segment densities near the chain center or the chain end in the concentration range up to 10% do not increase enough to interfere with the photoisomerization of the azobenzene label. However, the azobenzene label attached as a side group experiences some difficulty in photoisomerization even before C^* is reached. It is known that the chain dimension decreases with increasing concentration even before the overlap concentration is reached.² Therefore, the photoisomerization of a side group may be affected by the chain contraction, leading to an increase in segment density near a side group. As mentioned in the Introduction, Hayashi et al.⁷ found that the degree of TICT phenomenon increased linearly with the length of side chain in a good solvent while it leveled off in a poor solvent. This trend was explained by the chain contraction in a poor solvent. According to the calculation of Torkelson et al.,¹⁶ the azobenzene chromophore requires an extra volume of 127 Å³ in the vicinity of the probe for isomerization. This is a much larger volume (about 15 times) than that required for DMA to experience the TICT phenomenon. It is then not surprising that the side-labeled PS experiences some difficulty even below its C^* . Since the azo chromophore attached to polystyrene as a side group is dangling from the chain backbone, it responds most sensitively to the change of local segmental density due to the chain contraction.

In the concentration range above C^* , a strong site dependency of photoisomerization is observed. The α values decrease monotonically with increasing concentration except for the free probe where not much change was observed. As indicated in Figure 6, the chain entanglement concentration (C_e) for the free probe, EPS, and CPS is 23.2%, while it is 56.2% for SPS. The C_e was calculated by the following equation:¹⁷

$$C_e = M_e^0 \rho / M \quad (6)$$

where M_e^0 is the molecular weight between entanglements in a bulk polymer (18 000 for polystyrene), ρ is the polymer density, and M is the molecular weight of polymer. There is no abrupt change in α values at this concentration for the free probe, CPS, and EPS. For the SPS, the solution concentration does not extend above C_e . It is worth mentioning that the glass transition temperature (T_g) of a 50% polymer solution in toluene is about -100 °C. Therefore, the increase in T_g with increasing concentration has a negligible influence on the photoisomerization behavior up to 50% by weight.^{8a}

There are at least two factors which contribute to the increase of the segment density near the azobenzene chromophore above C^* . First, the chain contracts with increasing polymer concentration, and second, there are effects of intermolecular interactions or chain interpenetration. On the basis of the screening principle of Edwards¹ and de Gennes,¹⁸ it appears that chain dimensions should approach their unperturbed values for many systems as the polymer volume fractions approach 0.05–0.20, independent of molecular weight. According to Graessley's calculation¹⁹ based on the above argument, the concentration C^{**} over which the

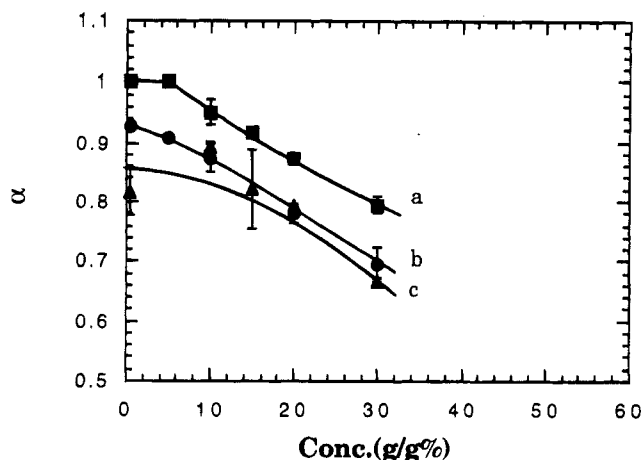


Figure 7. Changes of the fraction of the fast photoisomerization, α , as a function of concentration for the three labeled polystyrenes in cyclohexane at 34.8 °C: (a) E-PS; (b) C-PS; (c) S-PS.

dimensions may be regarded as remaining essentially constant for the polystyrene–toluene system is 12.8 g/dL corresponding to 15% by weight. Therefore, the effect of chain contraction with increasing concentration diminishes above 15% by weight, beyond which chain interpenetration dominates the segment-density increase.

Among three chain sites, the chain center is least affected by increasing concentration, as illustrated in Figure 6. This suggests that the microenvironment is less crowded near the chain center than near the other sites in the concentration range studied. As confirmed by the computer simulation (Figure 1), this may be due to the fact that the chain center is nearer to the center of mass, while the chain end is located much further from it. Thus, with increasing polymer concentration, the chain interpenetration starts from the outer shell of the chain dimension at which the chain end would be located with higher probability than would the chain center. Therefore, the chain center would be less crowded than the chain end with increasing concentration, as confirmed by the molecular simulation results (Figure 2b).

3. Photoisomerization in a Θ Solvent. All the characteristics of UV–visible spectra before irradiation for the three labeled polystyrenes in cyclohexane at 34.8 °C are quite similar to those for the corresponding samples in toluene. However, the photoisomerization behavior is quite different. Figure 7 shows the plot of α values as a function of concentration for the three labeled polystyrenes in cyclohexane at 34.8 °C.

Consider first the initial data point of each label. As indicated in α values, the nonlinearity in photoisomerization behavior is observed in the center and the side labels even in dilute solution. This can be explained by the congested environment in the Θ condition. From the computer simulation (Figure 2a), it was shown that the segment density in a dilute regime was much higher in the Θ condition than in a good solvent. This congestion is due to the chain contraction, as explained in the following paragraph. As shown in Table 4, the volume change due to the different nature of the solvent was calculated on the basis of the Flory–Fox viscosity relation²⁰ and the intrinsic viscosity data from the literature.²¹ From a rough calculation, it is shown that the volume of the chain in the Θ condition is shrunk to 36% or to 24% for the two different molecular weights. The side label shows the most dramatic change in the

Table 4. Intrinsic Viscosity of Polystyrene and the Percentage Volume Contraction Due to the Different Nature of the Solvent^a

	M_w		ref
	90 000	35 000	
$[\eta]$ (dL/g) (in toluene, 34.5 °C)	0.387	0.202	21
$[\eta]_\Theta$ (dL/g) (in cyclohexane, 34.5 °C)	0.246	0.153	21
$\alpha^3 = (\langle R_g^2 \rangle / \langle R_g^2 \rangle_\Theta)^{3/2} = [\eta] / [\eta]_\Theta$	1.573	1.320	20
ΔV (%) = $[(V_g - V_\Theta) / V_g] 100$ = $(1 - (1/\alpha^3)) 100$	36	24	

^a V_g = volume in toluene. ^b V_Θ = volume in cyclohexane.

α value due to the changing solvent even if the chain contraction was not greatest. Again, this result shows that the side chain is most sensitive to the chain contraction.

According to perturbation theory,¹¹ the change in the segment density due to the solvent power has a site dependency. The contraction of the polymer chain does not occur uniformly, but is greater in the outer shells than in the inner spaces. Therefore, the change in the microenvironment due to the solvent power is more severe in the vicinity of the chain ends than near the chain center. In dilute solution (the first data points), however, the chain ends in the Θ condition photoisomerize as fast as in the good solvent, while the chain center experiences some difficulty. Even with the more severe contraction in the Θ solvent, the chain ends may still have a much less congested environment than the chain center, as supported by lower segment density values in the chain ends than in the chain center in Figure 2a.

Consider now the concentration effect on α values. The α values decrease with increasing polymer concentration for all labels. In the Θ condition, the local segment density is affected only by the chain interpenetration since the chain dimension remains constant throughout the whole range of polymer concentrations. In that sense, the chain ends and chain centers seem to experience the chain interpenetration to a similar extent since α decreases with a similar slope for the two sites.

Another interesting result can be obtained by comparing the α values in the two solvents. The α values in toluene (good solvent) are always greater than in cyclohexane (Θ solvent). This reflects the lower segment density at a given concentration near any site in a good solvent. This was confirmed by computer simulation. It is interesting to compare this result with that of Chang and Morawetz^{6b} who found that the extent of chain interpenetration increased with increasing solvent power, as reflected by fluorescence energy transfer studies of mixtures of donor or acceptor tagged chains, suggesting that the lower segment density favored chain overlap in spite of the energetically unfavorable chain segment interaction. In our approach, however, photoisomerization of azobenzene is subject to the segment density in the vicinity of the chromophore. Both the intramolecular effect of chain contraction and the intermolecular effect of interpenetration affect the rate of photoisomerization. When the segment density is compared between a Θ solvent and a good solvent as in Figure 2a,b, it is greater up to 40% in the case of a Θ solvent. Therefore, it is reasonable to observe lower α values in a Θ solvent due to a more congested environment.²²

Acknowledgment. We acknowledge the financial support of this work by the National Science Founda-

tion, Polymer Program (Grant No. DMR 91-08060 and 94-15385), the Office of Naval Research, and the Army Research Office (Contract No. DAAL 03-92-G-0267). Y.S.K. acknowledges the Korean Government Scholarship for support of his graduate studies. The generous help provided by Mr. A. Glynn on computer simulation is also acknowledged. We also extend our gratitude to Professor H. Morawetz for his valuable help with the manuscript.

References and Notes

- (1) Edwards, S. F. *Proc. Phys. Soc.* **1966**, *88*, 265.
- (2) Daoud, M.; Cotton, J. P.; Farnoux, B.; Jannink, G.; Sarma, G.; Benoit, H.; Duplessix, R.; Picot, C.; de Gennes, P. G. *Macromolecules* **1975**, *8*, 804.
- (3) Richard, R. W.; Maconnachie, A.; Allen, G. *Polymer* **1978**, *19*, 266.
- (4) Takahashi, Y.; Isono, Y.; Noda, I.; Nagasawa, M. *Macromolecules* **1985**, *18*, 1002.
- (5) (a) Krause, W. A.; Kirste, R. G.; Haas, J.; Schmidt, B.; Stein, D. J. *Makromol. Chem.* **1976**, *177*, 1145. (b) Cotton, J. P.; Farnoux, B.; Jannink, G. J. *J. Chem. Phys.* **1972**, *57*, 290.
- (6) (a) Kirsh, Y. E.; Pavlova, N. R.; Kabanov, V. A. *Eur. Polym. J.* **1975**, *11*, 495. (b) Chang, L. P.; Morawetz, H. *Macromolecules* **1987**, *20*, 428. (c) Liao, T. P.; Morawetz, H. *Macromolecules* **1980**, *13*, 1228.
- (7) Hayashi, R.; Tazuke, S.; Frank, C. W. *Macromolecules* **1987**, *20*, 983.
- (8) (a) Lamarre, L.; Sung, C. S. P. *Macromolecules* **1983**, *16*, 1729. (b) Yu, W. C.; Sung, C. S. P.; Robertson, R. E. *Macromolecules* **1988**, *21*, 355. (c) Mita, I.; Horie, K.; Hirao, K. *Macromolecules* **1989**, *22*, 558.
- (9) Kim, Y. Private communication, Higher Dimension Research Inc., 1994.
- (10) Sung, C. S. P.; Gould, I. R.; Turro, N. J. *Macromolecules* **1984**, *17*, 1447.
- (11) Yamakawa, H. *Modern Theory of Polymer Solutions*; Harper & Row Publishers: New York, Evanston, San Francisco, and London, 1971.
- (12) Olaj, O. F.; Zifferer, G. *Makromol. Chem.* **1988**, *189*, 1097.
- (13) Williams, J. L. R.; Daly, R. C. *Prog. Polym. Sci.* **1977**, *5*, 61.
- (14) Zimmerman, G.; Chow, L. Y.; Paik, U. J. *J. Am. Chem. Soc.* **1958**, *80*, 3528.
- (15) (a) Adam, M.; Delsanti, M. *Macromolecules* **1977**, *10*, 1229. (b) Decker, D. Thesis, Strasbourg, 1968.
- (16) Victor, J. G.; Torkelson, J. M. *Macromolecules* **1987**, *20*, 2241.
- (17) (a) Graessley, W. W. *Adv. Polym. Sci.* **1974**, *16*, 1; **1982**, *47*, 67. (b) Ferry, J. D. *Viscoelastic Properties of Polymers*, 2nd ed.; Wiley: New York, 1970.
- (18) de Gennes, P. G. *Scaling Concepts in Polymer Physics*; Cornell University Press: Ithaca, NY, 1979; Chapter II.
- (19) Graessley, W. W. *Polymer* **1980**, *21*, 258.
- (20) Flory, P. J.; Fox, T. G. *J. Am. Chem. Soc.* **1951**, *73*, 1904.
- (21) Okada, R.; Toyoshima, Y.; Fujita, H. *Makromol. Chem.* **1963**, *59*, 137.
- (22) Waldow, D. A.; Johnson, B. S.; Hyde, P. D.; Ediger, M. D.; Kitano, T.; Ito, K. *Macromolecules* **1989**, *22*, 1345.

MA950502A